

# Monte Carlo Simulations of the One-Dimensional and Three-Dimensional Classical Heisenberg Models

Jim Hirschauer and William Ruddick

*University of Colorado at Boulder, Boulder, CO 80309-0390*

(Dated: May 1, 2004)

We review the analytical solution for the infinite spin (classical) Heisenberg model in one dimension. The partition function, internal energy, spin-spin correlation function, and zero-field susceptibility are shown. We compare these results to those of a Monte Carlo simulation in one dimension in order to confirm accuracy of the numerical solution. We also determine the zero-field magnetization and the magnetization as a function of field in the one dimensional simulation. We then use the simulation of the three-dimensional classical Heisenberg model to find critical behavior in the magnetization, zero-field magnetization, and susceptibility.

PACS numbers:

## I. INTRODUCTION

In 1925, E. Ising created a model of atomic spins which attempted to explain the phase transition of ferromagnets at the Curie temperature. The Ising model is a chain (one dimension) or lattice (two or three dimensions) of spins, and therefore magnetic moments, which can be in either of two orientations, up or down. The only interactions on the lattice are between nearest neighbor spins with parallel spins possessing an energy  $-J$  and antiparallel spins,  $+J$ . Ising also hoped this model would demonstrate a zero-field phase transition to ferromagnetic behavior at low temperatures. The simple solution of the one-dimensional problem revealed no critical behavior disappointing Ising who wrongly postulated that higher-dimensional models would also fail in that regard.

In 1928, W. Heisenberg applied the new quantum mechanics to this same problem, and invented a similar model using a vector coupling of the total quantum mechanical spin operators, still restricted to nearest neighbor interactions.[1] One can obtain a model of interacting classical spins by allowing the magnitude of the spin in this model to become infinite. The spin operators become normalized three dimensional vectors. The classical Heisenberg model is essentially the three-dimensional spin analogue of the one-dimensional spin Ising model, i.e. in the Ising model  $J = J_z$  and  $J_x = J_y = 0$  while in the classical (isotropic) Heisenberg model  $J = J_x = J_y = J_z$ .

Solutions to one-dimensional models are important not only because some physical systems can be modeled well in one dimension, but also as a comparison for numerical solutions that can then be generalized to higher dimensions.[2] In this way, we will show the accuracy of our simulation in one dimension by comparing it to accepted analytical solutions, and then obtain numerical results for the analytically insoluble three-dimensional model.

## II. ANALYTICAL SOLUTION TO THE ONE-DIMENSIONAL CLASSICAL HEISENBERG MODEL

We present a short review of the exact solution in one dimension.[3] The hamiltonian for the classical Heisenberg chain of  $N$  spins in a magnetic field  $\mathbf{H}$  is

$$\mathcal{H} = -J \sum_{i=1}^N \mathbf{s}_i \cdot \mathbf{s}_{i-1} - \mu \sum_{i=1}^N \mathbf{H} \cdot \mathbf{s}_i. \quad (1)$$

Where  $\mu$  is the magnetic moment and  $J$  is the spin-spin coupling constant. Clearly,  $J$  is positive for a ferromagnet, negative for an anti-ferromagnet, and zero for a paramagnet. In the ferromagnetic case, with which we are primarily concerned, the spins minimize energy by aligning with their nearest neighbors and the field. Letting

$$K = J/k_B T, \quad (2)$$

the zero field partition function is

$$\mathcal{Z}_N = \int \frac{d\Omega_0}{4\pi} \dots \int \frac{d\Omega_N}{4\pi} \exp[K \sum_{i=1}^N \mathbf{s}_i \cdot \mathbf{s}_{i-1}]. \quad (3)$$

If the polar coordinates of the  $i$ th spin vector are taken to be the polar axis of the  $(i-1)$ th spin in each integral in Eq. (3) then the integrals separate and

$$\mathcal{Z}_N = \int \frac{d\Omega_0}{4\pi} \prod_{i=1}^N \int_0^\pi \frac{1}{2} e^{K \cos \theta_i} \sin \theta_i d\theta_i. \quad (4)$$

Now the partition function reads

$$\mathcal{Z}_N = \left[ \frac{\sinh K}{K} \right]^N. \quad (5)$$

In the thermodynamic limit  $N \rightarrow \infty$ , this partition function for the open chain of  $N$  spins agrees with that obtained for a ring of  $N$  spins, as one would expect.[4] The zero field internal energy, Fig. 1, is

$$\frac{U}{NJ} = \frac{\partial}{\partial \beta} (\ln \sinh K - \ln K) \quad (6)$$

$$= \frac{1}{K} - \coth K. \quad (7)$$

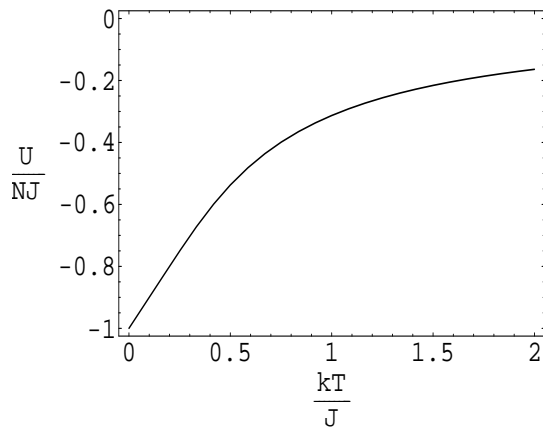


FIG. 1: The analytical zero-field internal energy per particle (scaled by  $J$ ) versus temperature. The linearity of the internal energy for low temperature is explained later.

The spin-spin correlation function is defined

$$g_i(R) = \langle \mathbf{s}_i \cdot \mathbf{s}_{i+R} \rangle = 3 \langle s_{i,z} s_{i+R,z} \rangle, \quad (8)$$

$$= 3 \mathcal{Z}_{\mathcal{N}}^{-1} \int \frac{d\Omega_0}{4\pi} \dots \int \frac{d\Omega_N}{4\pi} s_{i,z} s_{i+R,z} \times e^{-\beta \mathcal{H}\{\mathbf{s}_i\}}, \quad (9)$$

and can be determined using a procedure similar to that for the partition function. However, in this case, only the first  $i$  and last  $N-i+R$  integrals can be separated, and the remaining  $R$  integrals are computed using a somewhat complicated approach.[5] With the numerical solution of these models being our focus, we will not investigate that approach here. Nevertheless, the correlation function is found to be

$$g_i(R) = [u(K)]^{|R|}, \quad (10)$$

where  $u(K)$  is the Langevin function  $\coth K - \frac{1}{K}$ [4]. Notice that  $|u(K)| \leq 1$ , and so the correlation drops off exponentially as  $R$  increases, i.e. the farther spins are from one another the less they are correlated, as one would expect.

The zero-field susceptibility, Fig. 2, is found from this correlation function, for large  $N$  and  $T \neq 0$ , to be

$$\chi_0(T) = \frac{N\mu^2}{3k_B T} \frac{1 + u(K)}{1 - u(K)}. \quad (11)$$

### III. MONTE CARLO SIMULATION

We performed a Monte Carlo simulation using the Metropolis algorithm for a system of  $N$  classical, unit vectors with periodic boundary conditions. As noted above, the solutions for a ring and an open chain are identical in the thermodynamic limit.

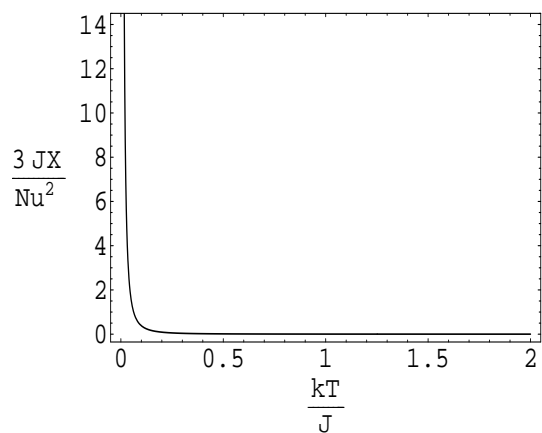


FIG. 2: The analytical zero-field susceptibility versus temperature; in the one-dimensional case there is no critical behavior other than at  $T = 0$ .

The Metropolis algorithm is widely used to simulate a number of systems such as spin, scalar field theories, and gauge theories, because of its simplicity. As is the case in most Monte Carlo algorithms, the Metropolis algorithm begins with, in our case, a pseudo-random (random) configuration of the system and evolves this initial state and all of its successors by making random, small changes to system variables.

A system, in our case, of spins,  $\{s_i\}$ , is altered by changing a single element  $s_i + \epsilon \rightarrow s'_i$ , and then accepting the new system  $\{s'_i\}$  if the new energy  $E'$  is less than the previous  $E$  or else with a probability of  $e^{-\beta(E'-E)}$ . [6] This process is repeated for all other elements in the array; one attempted change of each element in the array is considered one Monte Carlo step (MCS).

In our simulation we changed the  $x$ ,  $y$ , and  $z$  components of each array element by a random length  $l$ , with  $-\epsilon \leq l \leq +\epsilon$  for a tunable simulation parameter  $\epsilon$ . We then renormalized the vector and checked its new energy as described.

After a number of MCS, the system relaxes into a low energy equilibrium state which is completely uncorrelated to the initial configuration and about which it will make only small fluctuations. Once equilibrium is reached one begins sampling the system for any relevant data, in our case, energy and spin.

#### A. Simulation Optimization

We increased the precision of our simulation by varying the size of our random, small change  $\epsilon$ , and in effect our correlation time  $\tau$ . We also maximized the number of samples taken at equilibrium  $M$ . If the time correlation function,  $\phi$  for any thermodynamic quantity  $A$  can be written

$$\phi(t) = \frac{\langle A(t)A(0) \rangle - \langle A(t) \rangle \langle A(0) \rangle}{\langle A^2 \rangle - \langle A \rangle^2}, \quad (12)$$

then the correlation time  $\tau$ , with  $T_0$  being the first time that  $\phi(t) < 0$ , is

$$\tau \simeq \sum_{i=1}^{T_0} \phi(i). \quad (13)$$

The correlation time shows how correlated two configurations are in a simulation. For a large  $\tau$ , two system states separated by many MCS are still highly correlated. This clearly has a significant effect on the validity of any results; and even more precisely, the uncertainty in any measurement of an observable scales as  $\sqrt{\frac{2\tau+1}{M}}$ . Ideally, one would make  $\tau$  arbitrarily small while maximizing  $M$ , but these parameters are tied to our only tunable parameter  $\epsilon$  in a way that makes such a strategy impossible. Additionally, minimizing  $\tau$ , even without regard for  $M$ , is not as straightforward as it seems.

A simulation with  $\epsilon$  too small will take many MCS to reach equilibrium, thereby making a large sample difficult to obtain. Furthermore, an arbitrarily small  $\epsilon$  does not imply an arbitrarily small  $\tau$ . As  $\epsilon$  gets too small the configurations can change only very little from step to step, making successive MCS very correlated.

An  $\epsilon$  too large will result in a large  $\tau$ , but will very quickly reach equilibrium making a large  $M$  easy to obtain. By looking at plots of the correlation function for different  $\epsilon$  at several temperatures, Fig. 3, we empirically determined that a value of  $\epsilon \simeq .6$  minimizes  $\tau$ . We also ran each simulation as long as feasible to increase  $M$  and minimize  $\sqrt{\frac{2\tau+1}{M}}$ .

Another concern was when to begin making measurements on the system, or how to determine when the system had reached equilibrium. Several different automated methods were attempted to tell the program when (after how many MCS) to start sampling the data. However, because this determination depended sensitively on other parameters such as temperature, field, and  $\epsilon$ , we ultimately found it easiest to run a short simulation, visually inspect the energy data for a point just beyond equilibrium, and use this as our initial sampling spot in the following simulations.

We also greatly improved this aspect of the simulation by using an equilibrated sample from the end of a previous simulation as the starting configuration for a new simulation, although we still waited the empirically determined number of MCS before sampling to ensure that configuration correlation had gone to zero.

## B. Simulation of the One-Dimensional Ring

For the simulation of the 1-D, zero-field Heisenberg ring of 50 spins, the energy check for each new array

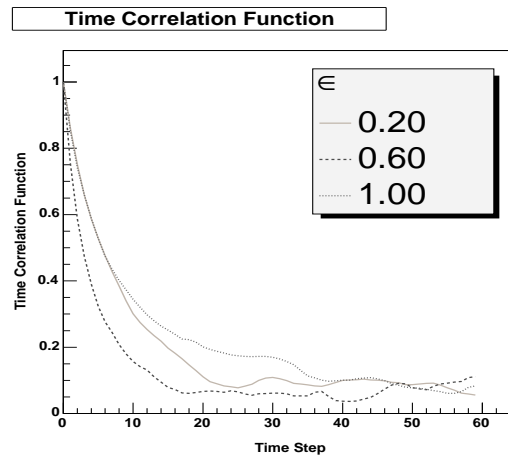


FIG. 3: The time correlation function versus MCS at  $\frac{k_B T}{J} = 1.5$ . The correlation time is the area under each curve. This area is minimized at  $\epsilon = 0.6$ . The optimal  $\epsilon$  depends weakly on temperature near the critical point; small fluctuations in  $\tau$  were negligible due to large samples,  $M \simeq 20,000$ , gathered during simulations for final results.

configuration was merely a matter of checking interactions with nearest neighbors, left and right, along the chain. While no critical behavior was expected for temperatures above  $T = 0$ , we were eager to measure results that agreed with the analytically determined properties shown above.

The only information sampled from the simulation was the spin and energy of each site on the chain,  $\mathbf{s}_i$  and  $E_i$ . From this we were able to calculate the average spin of the system in a certain direction, say  $z$ ,  $\langle \mathbf{s}_z \rangle$ , the spin-spin correlation function  $\langle s_{0,z} s_{0+R,z} \rangle$  and the energy per particle; and from these the magnetization, susceptibility, and internal energy.

When finding quantities in zero-field that require a “reference” spin or a preferred direction (called the  $z$ -direction) such as the magnetization or pair correlation function, the  $z$ -direction was taken to be the direction of the first spin vector in the configuration (after the system has reached equilibrium). In the case of the pair correlation function the spin of the initial configuration was used as  $s_i$ . The pair correlation function behaves just as predicted analytically in Eq. 10. The correlation of any two spins on the chain,  $g_i(R)$ , falls exponentially as the distance between them  $R$ , Fig. 4.

To determine the behavior of the ring as a function of temperature or field, we simply ran a series of simulations stepping through different values of the parameter calculating the interesting quantity at each value. Two such quantities are the internal energy and the zero-field susceptibility as functions of temperature.

The internal energy is linear for low  $T$  due to the equipartition theorem,  $\frac{U}{N} = \frac{1}{2} k_B T \times qd$  where  $qd$  is the number of quadratic degrees of freedom of the hamiltonian. The Heisenberg hamiltonian is essentially the scalar product of two unit vectors,  $s_i$  and  $s_{i-1}$ , charac-

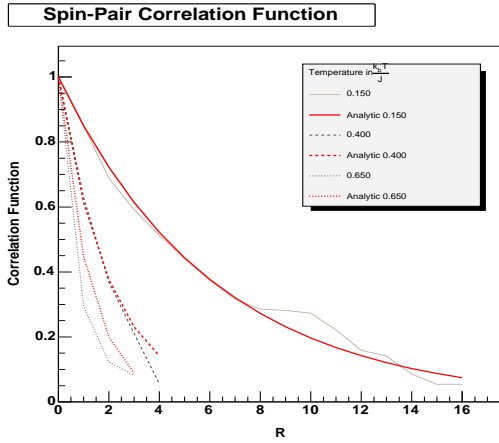


FIG. 4: Spin-spin correlation function versus distance along the ring for several temperatures. The correlation is predicted to fall exponentially with distance; numeric correlation functions decay exponentially, but fluctuate much than we would prefer. As we expected, high temperature correlations drop to zero faster than low temperature correlations.

terized by angles  $\theta_i$ ,  $\phi_i$ ,  $\theta_{i-1}$ , and  $\phi_{i-1}$ . This hamiltonian contains the term  $\cos \phi_i \times \cos \theta_i$ , which in the low temperature expansion can be written  $1 - \theta_i^2 - \phi_i^2$ . [5] Two quadratic degrees of freedom, at low temperature, result in the direct variation of the internal energy with temperature,  $\frac{U}{N} = k_B T$ . The linearity and agreement with theory of the internal energy are both apparent in Fig. 5

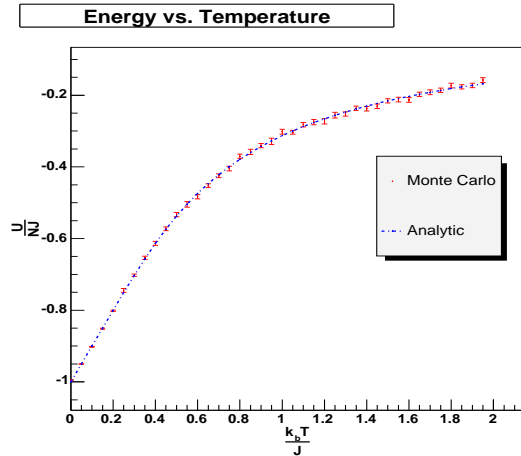


FIG. 5: The internal energy versus temperature for the 1-D Heisenberg ring agrees very well with the theoretical prediction.

The susceptibility was calculated from the simulation as

$$\chi_0 = \left\langle \frac{2}{N^2} \sum_{R=1}^{N/2} \sum_{i=0}^N \mathbf{s}_i \cdot \mathbf{s}_{i+R} \right\rangle. \quad (14)$$

Periodic boundary conditions assured that these sums

were over sites on the array that made sense to simulation, i.e. sites that exist. The zero-field susceptibility diverges as  $T \rightarrow 0$  in the theory and simulation as shown in Fig. 6.

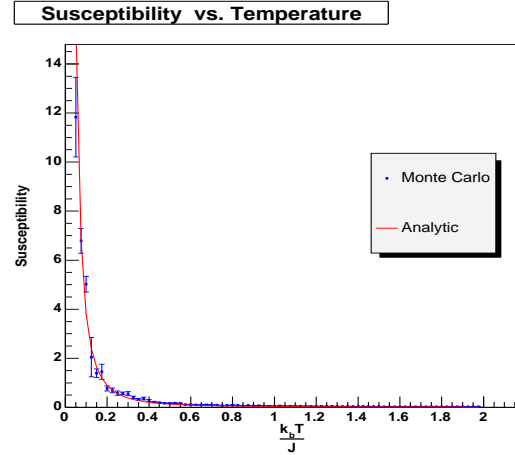


FIG. 6: The zero-field susceptibility versus temperature displays no critical behavior for  $T \neq 0$  in one dimension, but agrees very well with the theory.

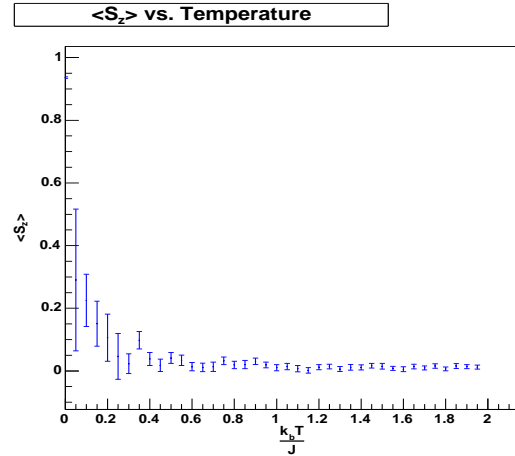


FIG. 7: The zero-field magnetization versus temperature in one dimension also displays no phase transition, but is interesting as a comparison for the 3-D case.

Having determined that the spin-spin correlation function, internal energy, and susceptibility all behave as predicted analytically, we calculated the magnetization versus temperature and field, Figs. 7 and 8, respectively, in anticipation of the critical behavior of these quantities in three dimensions. The magnetization was calculated as  $M = \langle \sum_{i=1}^N s_{i,z} \rangle$  where, again, the z-direction in the zero-field case was taken as the spin direction of the first vector measured in each configuration.

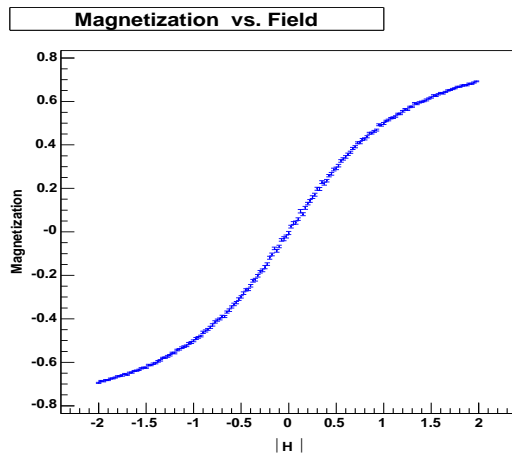


FIG. 8: The magnetization versus field in one dimension at  $T = 1K$ .

### C. Simulation in Three Dimensions and Critical Behavior

The simulation of the 3-D array with periodic boundary was very similar to that of the 1-D ring, except nearest neighbor interactions involved six neighbors rather than two. The simulation was run on a  $10 \times 10 \times 10$  array with periodic boundary conditions. We were particularly interested in the three dimensional simulation in order to observe the phase transitions and critical temperatures of the magnetization and susceptibility.

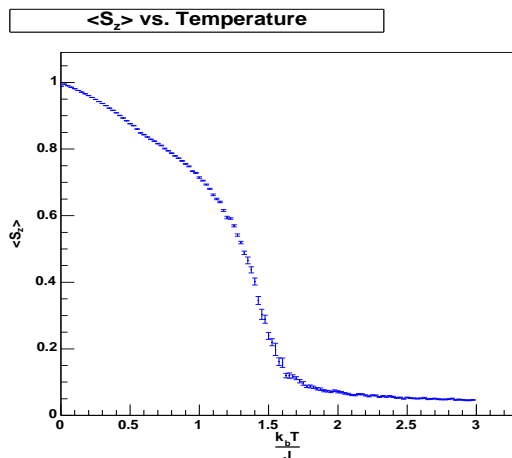


FIG. 9: The zero-field magnetization versus temperature shows a phase transition in three dimensions with a critical temperature  $\frac{kT_c}{J} \simeq 1.6$ . This transition would be infinitely sharp in the thermodynamic limit.

For low  $T$ , the zero-field magnetization, Fig. 9, is linear. This is also due to equipartition[7]; in low temperature the spins are aligned, and again, the cosines in the Hamiltonian can be taken as the first two terms of their Taylor expansions. This will again result in two squared degrees of freedom in the Hamiltonian and linearity in

the related quantities.

The susceptibility and magnetization were calculated just as in one dimension, but again,  $\mathbf{s}_i \cdot \mathbf{s}_{i+R}$  in Eq. 14 refers to six interactions rather than two. The zero-field susceptibility and magnetization versus field, Figs. 10 and 11, respectively, also show phase transitions in three dimensions, as expected, with a critical temperature of  $\frac{kT_c}{J} \simeq 1.6$ . The susceptibility clearly peaks at  $\frac{kT_c}{J}$ , but it does not truly diverge because these simulations were performed on a  $10 \times 10 \times 10$  array. Though this is a large array to simulate, in terms of CPU time, it is by no means approaching the thermodynamic limit. The small size of the array likewise dulls the sharpness of the phase transition in the magnetization.

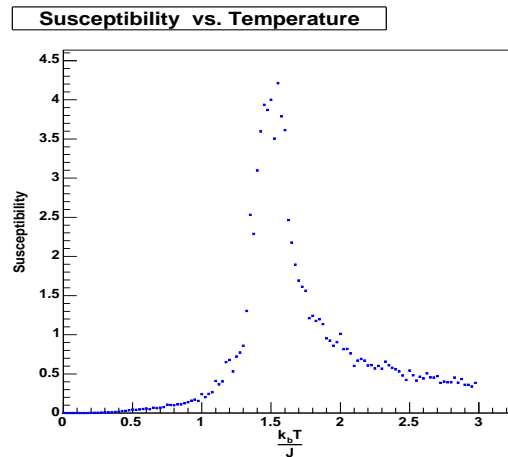


FIG. 10: The zero-field susceptibility versus temperature exhibits criticality at a temperature, again  $\frac{kT_c}{J} \simeq 1.6$ , that agrees very well with that of the zero-field magnetization, Fig. 9.

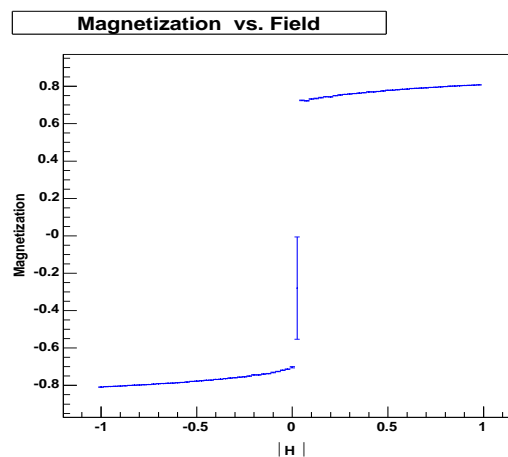


FIG. 11: The magnetization versus field in three dimensions has infinite slope at  $T = 1K$  as opposed to the smooth curve for the quantity in one dimension, Fig. 8.

#### IV. CONCLUSIONS

The Classical Heisenberg Model is a valuable tool in the study of critical phenomena. Its exact solution in one dimension is useful as a model for several one dimensional systems. It can be simulated accurately in one dimension by using the simple Metropolis Monte Carlo algorithm, and the one-dimensional case can be generalized to higher dimensions where interesting critical behavior occurs.

We have presented an analytical solution to the One-Dimensional Classical Heisenberg Model, and performed a Monte Carlo simulation of the model in one and three dimensions. Theoretical predictions for the energy, magnetization, and susceptibility in one dimension coincided with results obtained from the simulation. No phase

transitions were observed in the one-dimensional model, but the three-dimensional model exhibited criticality in the variable-field and zero-field magnetization as well as zero-field susceptibility; all with critical temperature  $\frac{kT_c}{J} \simeq 1.6$ .

An interesting expansion of this Monte Carlo approach to the isotropic,  $J = J_x = J_y = J_z$ , Heisenberg model would be to consider the anisotropic model with  $J_x \neq J_y \neq J_z$ , or probably  $J_x = J_y \neq J_z$ . The anisotropic model is also exactly soluble in one dimension, but its behavior differs largely from the isotropic model at low temperature.[8] Monte Carlo simulations in three dimensions could reveal interesting differences between the two models in critical behavior or in general.

- 
- [1] L. B. et al., *Twentieth Century Physics, Volume I* (Institute of Physics Publishing and American Institute of Physics Press, 1995).
  - [2] H. E. Stanley, *Phys. Rev. Lett.* **179**, 570 (1968).
  - [3] M. E. Fisher, *Am. J. Phys.* **32**, 343 (1964).
  - [4] G. S. Joyce, *Phys. Rev. Lett.* **155**, 478 (1966).
  - [5] D. Hudson and J. Peoble, Term Paper (2004).
  - [6] K. Binder and D. Heerman, *Monte Carlo Simulations in Statistical Physics* (Spring-Verlag, 1992).
  - [7] P. Beale, private communication, 2004.
  - [8] G. S. Joyce, *Phys. Rev. Lett.* **19** (1967).
  - [9] R. Niclasen, Master's thesis, University of Copenhagen, Copenhagen, Denmark (2001).
  - [10] G. F. Mazenko, *Equilibrium Statistical Mechanics* (John Wiley and Sons, Inc., 2000).
  - [11] W. G. et al., *Thermodynamics and Statistical Mechanics* (Springer, 1995).